

A Purine-like Nickel(II) Base Pair for DNA**

Christopher Switzer,* Surajit Sinha, Paul H. Kim, and Benjamin D. Heuberger

Nucleic acids rely on complementary functionalized purine and pyrimidine heterocycles to encode genetic information as G·C and A·T(U) base pairs. Several approaches have been developed to expand the number of available base pairs beyond the two natural pairs, including the use of non-standard hydrogen-bond donor/acceptor patterns,^[1] van der Waals and hydrophobic interactions,^[2] and metal coordination.^[3] Herein we report the realization of a naturally inspired metallo base pair with a purine core whose design derives from minimal modification of adenine. The resulting base pair (Pur^P·Ni·Pur^P, Figure 1) is found to have the following novel features and properties: 1) greater stability than a G·C base pair, 2) a surprising dimensional resemblance to natural purine–pyrimidine base pairs, and 3) the potential to serve in an ion-activated switch.

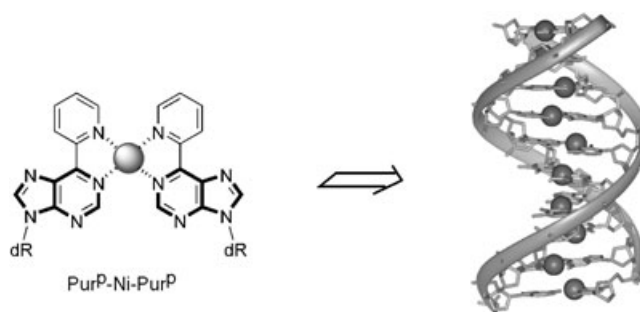
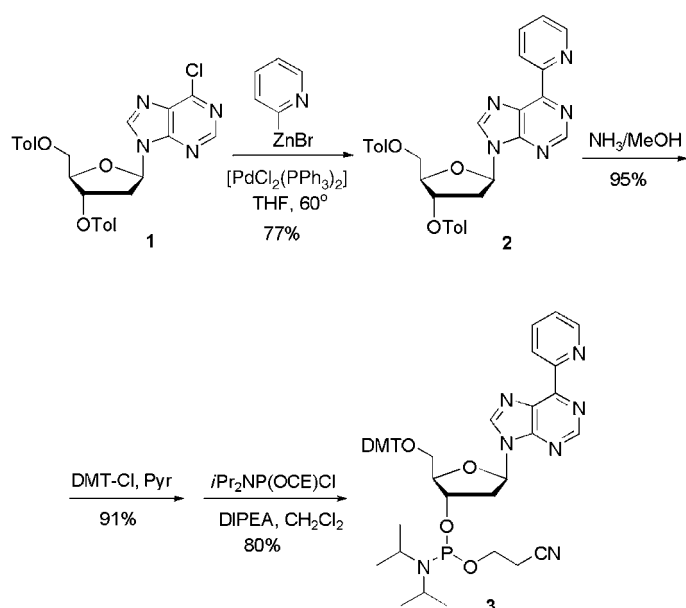


Figure 1. Left: The 6-(2'-pyridyl)-purine (Pur^P) metallo base pair. Right: A representation of a hypothetical helix composed of purely Pur^P·Ni²⁺·Pur^P base pairs.

Formally, Pur^P is derived from adenine by replacing the 6-amino group with a pyridyl group. This functional-group interchange places two Lewis basic donor atoms (the purine N1 and pyridine N1' atoms) in an optimal 1,4-relationship for coordinating metal ions. Scheme 1 summarizes the synthesis of Pur^P. The key transformation involved a modified Negishi coupling of pyridyl zinc bromide with chloropurine deoxyriboside **1**^[4] to provide pyridylpurine deoxyriboside **2**. We

[*] Prof. C. Switzer, S. Sinha, P. H. Kim, B. D. Heuberger
Department of Chemistry
University of California
Riverside, CA 92521 (USA)
Fax: (+1) 951-787-2435
E-mail: christopher.switzer@ucr.edu

[**] This work was supported by DOD/DARPA/DMEA under award no. DMEA90-02-2-0216 and the NASA exobiology program under award no. NAG5-9812.



Scheme 1. Synthesis of 2'-deoxyribosyl-N9-[6-(2'-pyridyl)-purine] phosphoramidite **3**. Tol = 4-toluoyl, THF = tetrahydrofuran, DMT = 4,4'-dimethoxytriphenylmethyl, Pyr = pyridine, OCE = cyanoethyl, DIPEA = *N,N*-diisopropylethylamine.

initially used the conditions reported for the preparation of ribosyl and acyclic analogues of **2**^[5] but found that an improved yield was possible by switching to a $[\text{PdCl}_2(\text{PPh}_3)_2]$ catalyst.^[6] Pyridylpurine nucleoside **2** was transformed in three steps into phosphoramidite **3**. DNA containing Pur^{P} was prepared by using **3** and standard phosphite triester methodology on an ABI394 synthesizer. Complementary dodecamer DNA strands were prepared, each bearing a single Pur^{P} residue: 5'-d-CTTTCT Pur^{P} TCCCT (**4**) and 5'-d-AGGGAP ur^{P} AGAAAG (**5**). These oligomers were purified by PAGE, and their identities were confirmed by MALDI mass spectrometry.

To assess the viability of Pur^{P} as the organic component of a metallo base pair, UV-monitored thermal denaturation of complementary dodecamers **4** and **5** bearing single Pur^{P} residues was performed in the presence of the divalent ions noted in Table 1. Representative denaturation profiles are shown in Figure 2. In all, nine divalent metal ions were screened for their abilities to coordinate to the $\text{Pur}^{\text{P}}\cdot\text{Pur}^{\text{P}}$ site contained in the **4/5** duplex by measuring the T_{m} value; the T_{m} value of a metal-free control with the same duplex (Table 1, entry 11) was also recorded. As is apparent from the table, only four of the seven divalent ions gave T_{m} values for **4/5** that differed significantly from the metal-free control: Ni^{2+} , Co^{2+} , Cu^{2+} , Zn^{2+} , and Ag^{+} . Of these five metals, Ni^{2+} is the most stabilizing. $\text{Pur}^{\text{P}}\cdot\text{Co}^{2+}\cdot\text{Pur}^{\text{P}}$ leads to a duplex T_{m} value roughly in between those of the **6/10** and **7/11** duplexes bearing T·A and C·G pairs, respectively. More significantly, the $\text{Pur}^{\text{P}}\cdot\text{Ni}^{2+}\cdot\text{Pur}^{\text{P}}$ base pair is more stabilizing to a double helix than a C·G base pair by a margin of 6°C under the conditions reported in Table 1, with 5 μM NiCl_2 . Importantly, the $\text{Pur}^{\text{P}}\cdot\text{Pur}^{\text{P}}$ **4/5** duplex is highly destabilized in the absence of Ni^{2+} or other

Table 1: DNA-duplex melting temperatures, T_{m} , in the presence and absence of divalent ions.^[a]

5'-d-CTTTCT Pur^{P} TCCCT

3'-d-GAAAGAP ur^{P} AGGGA

Entry	X·Y	Duplex	Metal	T_{m}	Δ ^[b]
1	$\text{Pur}^{\text{P}}\cdot\text{Pur}^{\text{P}}$	4/5	NiCl_2	46.1	+6.0
2	$\text{Pur}^{\text{P}}\cdot\text{Pur}^{\text{P}}$	4/5	$\text{Ni}(\text{NO}_3)_2$	46.6	+6.5
3	$\text{Pur}^{\text{P}}\cdot\text{Pur}^{\text{P}}$	4/5	CoCl_2	38.8	-1.3
4	$\text{Pur}^{\text{P}}\cdot\text{Pur}^{\text{P}}$	4/5	CuCl_2	31.4	-8.7
5	$\text{Pur}^{\text{P}}\cdot\text{Pur}^{\text{P}}$	4/5	ZnSO_4	30.8	-9.3
6	$\text{Pur}^{\text{P}}\cdot\text{Pur}^{\text{P}}$	4/5	AgNO_3	30.5	-9.6
7	$\text{Pur}^{\text{P}}\cdot\text{Pur}^{\text{P}}$	4/5	FeSO_4	28.8	-11.3
8	$\text{Pur}^{\text{P}}\cdot\text{Pur}^{\text{P}}$	4/5	MnCl_2	29.2	-10.9
9	$\text{Pur}^{\text{P}}\cdot\text{Pur}^{\text{P}}$	4/5	$\text{Eu}(\text{NO}_3)_3$	29.1	-11.0
10	$\text{Pur}^{\text{P}}\cdot\text{Pur}^{\text{P}}$	4/5	$\text{Pd}(\text{NO}_3)_2$	27.3	-12.8
11	$\text{Pur}^{\text{P}}\cdot\text{Pur}^{\text{P}}$	4/5	— ^[c]	28.5	-11.6
12	T· Pur^{P}	6/5	NiCl_2	27.1	-13.0
13	C· Pur^{P}	7/5	NiCl_2	26.6	-13.5
14	A· Pur^{P}	8/5	NiCl_2	27.0	-13.1
15	G· Pur^{P}	9/5	NiCl_2	29.1	-11.0
16	T·A	6/10	— ^[c]	36.8	-3.3
17	T·A	6/10	NiCl_2 ^[d]	37.4	-2.7
18	T·A	6/10	CoCl_2 ^[d]	36.7	-3.4
19	C·G	7/11	— ^[c]	40.2	+0.1
20	C·G	7/11	NiCl_2 ^[d]	40.1	0.0
21	C·G	7/11	CoCl_2 ^[d]	39.9	-0.2

[a] Samples contained 2.5 μM of each DNA strand, 5 μM divalent ion where indicated, 50 mM NaCl, and 10 mM NaH_2PO_4 (pH 7.0). All measurements were performed at least in triplicate. [b] Difference in T_{m} value relative to that of duplex **7/11** (X·Y = C·G) in the presence of NiCl_2 (entry 20). [c] No divalent metal ions were added. [d] Divalent ion was added in these cases as a control.

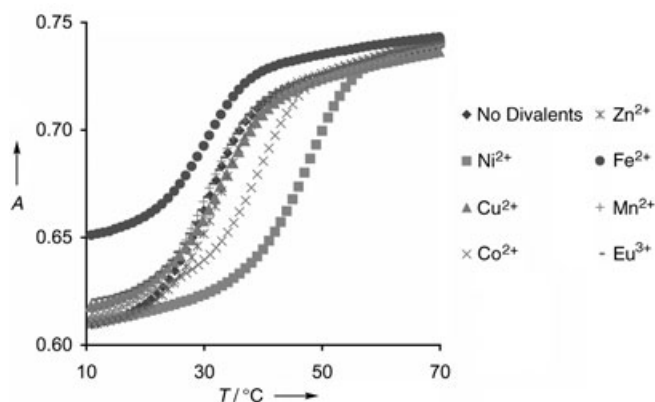


Figure 2. Absorbance versus temperature denaturation profiles. Conditions are as reported in Table 1.

divalent ions (Table 1, entry 11): there is a -17.6°C difference in T_{m} value between the $\text{Pur}^{\text{P}}\cdot\text{Ni}^{2+}\cdot\text{Pur}^{\text{P}}$ ($T_{\text{m}} = 46.1^\circ\text{C}$) and $\text{Pur}^{\text{P}}\cdot\text{Pur}^{\text{P}}$ ($T_{\text{m}} = 28.5^\circ\text{C}$) base pairs (Table 1, entry 1 versus entry 11). As a control, both the T·A **6/10** and the C·G **7/11** duplexes were denatured in the presence and absence of Ni^{2+} or Co^{2+} , and no significant changes were observed in the T_{m} values (Table 1, entries 16–21).

The stability of mismatches between the four natural bases and Pur^{P} was investigated in the presence of Ni^{2+}

(Table 1, entries 12–15). Clearly, none of the natural bases make stable pairs with $\text{Pur}^{\text{P}}\cdot\text{Ni}^{2+}$. Indeed, the ΔT_{m} values of the mismatched pairs relative to the $\text{Pur}^{\text{P}}\cdot\text{Ni}^{2+}\cdot\text{Pur}^{\text{P}}$ base pair (not the Δ values listed in Table 1 which are relative to the C-G pair) range from -17 to -19.5°C . By contrast, T-G and C-A mismatches of the parent natural duplex under the same conditions show ΔT_{m} values of -7.4 and -18.5°C under the same conditions.^[7] Thus, all four $\text{Pur}^{\text{P}}\cdot\text{Ni}^{2+}$ mismatches with natural bases are much less stable than the $\text{Pur}^{\text{P}}\cdot\text{Ni}^{2+}\cdot\text{Pur}^{\text{P}}$ match. A further point to note is that the instabilities seen for all four $\text{Pur}^{\text{P}}\cdot\text{Ni}^{2+}$ mismatches with natural bases rival the most severe natural nucleobase mismatches such as C-A.

Within the double helix, three possible geometries could be envisioned for divalent metal ion complexation by Pur_2^{P} : square planar, tetrahedral, and D_2^{d} (a geometry intermediate between square planar and tetrahedral). In the absence of a geometric preference by the metal ion, the most productive geometry for a metallo base pair in forming the double helix is expected to be square planar because this will maximize favorable nearest-neighbor stacking interactions. Low-energy square-planar geometries should be accessible for Ni^{2+} , Co^{2+} , Cu^{2+} , Ag^{+} , and Pd^{2+} ions. The first two of these five ions appreciably stabilize the Pur_2^{P} -bearing helix, whereas the latter three do not. As a result, it may be concluded that geometry alone is an insufficient predictor of metal-ion affinity for Pur^{P} . A circular dichroism spectrum of duplex **4/5** in the presence of Ni^{2+} is consistent with a B-DNA structure.

To assess the viability of a square-planar geometry for $\text{Pur}^{\text{P}}\cdot\text{Ni}^{2+}\cdot\text{Pur}^{\text{P}}$, an ab initio geometry optimization was performed on the complex by using Gaussian98^[8] at the B3LYP/6-31G*(CHN)/SDD(Ni) level of theory. Figure 3 (left panel) shows the square-planar geometry found to be a (local) minimum on the energy surface. Interestingly, this structure bears an N9–N9' (purine numbering) $\text{Pur}^{\text{P}}\text{--}\text{Pur}^{\text{P}}$ distance of 9.54 \AA , which nearly replicates the N9–N1 purine–pyrimidine distance of 9.05 \AA that occurs in natural B-DNA helices for both G-C and A-T base pairs. This suggests $\text{Pur}^{\text{P}}\cdot\text{Ni}^{2+}\cdot\text{Pur}^{\text{P}}$ is a good dimensional mimic of natural base pairs despite the fact that the metallo base pair incorporates two purine-like components. Superposition of ab initio optimized $\text{Pur}^{\text{P}}\cdot\text{Ni}^{2+}\cdot\text{Pur}^{\text{P}}$ and A-T base-pair structures (Figure 3, right panel) further supports this idea and shows that Pur^{P} coordination of Ni^{2+} is attended by rotation of the Pur^{P}

bases towards the major groove, with a corresponding shortening of the distance between interstrand N9 atoms.

The $\text{Pur}^{\text{P}}\cdot\text{Ni}^{2+}\cdot\text{Pur}^{\text{P}}$ structure in Figure 3 results from head-to-head dimerization ($\text{N1},\text{N1}'\text{--}\text{Pur}^{\text{P}}\cdot\text{Ni}^{2+}\cdot\text{N1},\text{N1}'\text{--}\text{Pur}^{\text{P}}$). An alternative head-to-tail dimerization mode of Pur^{P} ($\text{N1},\text{N1}'\text{--}\text{Pur}^{\text{P}}\cdot\text{Ni}^{2+}\cdot\text{N7},\text{N1}'\text{--}\text{Pur}^{\text{P}}$) was also investigated computationally. The geometry of this latter complex was found to be highly nonplanar due to ligand encroachment resulting from the 1,5-relationship of the nitrogen atoms ($\text{N7},\text{N1}'$) presented by the “tail”-oriented Pur^{P} . (In contrast, the opposing “head”-oriented Pur^{P} bears the optimal 1,4-relationship of nitrogen atoms, as found in bipyridine.) Therefore, the head-to-tail dimer is predicted to be less compatible with a helix than the head-to-head dimer.

Metallo base pairs could become functional elements of oligonucleotides that activate or suppress enzymatic activity (for example, transcription or translation) in the presence or absence of a metal ion. For a proof of principle, we have incorporated three consecutive Pur^{P} residues into a helix to attain “on” and “off” states (in the presence and absence of Ni^{2+} , respectively) that are sufficiently insulated from one another to be effectively binary (0 or 1). The following tetradecamer DNA strands were prepared: 5'-d-CTTCTCT Pur^{P} Pur^{P} Pur^{P} TCCCT (**12**) and 5'-d-AGGGAP ur^{P} ur^{P} AGAAAG (**13**). Gratifyingly, the T_{m} values for the **12/13** duplex under the conditions reported in Table 1 were 64.3°C in the presence of $10.0\text{ }\mu\text{M}$ NiCl_2 (1.3 equiv per Pur^{P} residue) and 20.6°C in the absence of Ni^{2+} . Thus, the T_{m} values between the “on” (Ni^{2+} present) and “off” (Ni^{2+} absent) states of this system are separated by 43.7°C , a difference sufficient to produce binary behavior at 37°C (that is, at this temperature, in the presence of Ni^{2+} the helix is present and in the absence of Ni^{2+} the helix is absent).

In summary, Pur^{P} leads to a metallo base pair with Ni^{2+} selectivity that is more stable than natural G-C and A-T base pairs. Additionally, $\text{Pur}^{\text{P}}\cdot\text{Ni}^{2+}\cdot\text{Pur}^{\text{P}}$ is orthogonal in its pairing properties relative to the four genomic nucleobases: all mismatches are highly destabilizing to the helix in comparison to the parent metallo base pair. Finally, $\text{Pur}^{\text{P}}\cdot\text{Ni}^{2+}\cdot\text{Pur}^{\text{P}}$ appears to resemble natural base pairs dimensionally and has the potential to serve as the functional component of an ion-activated switch. Given the resemblance between natural purines and Pur^{P} it is possible that enzymes, including those

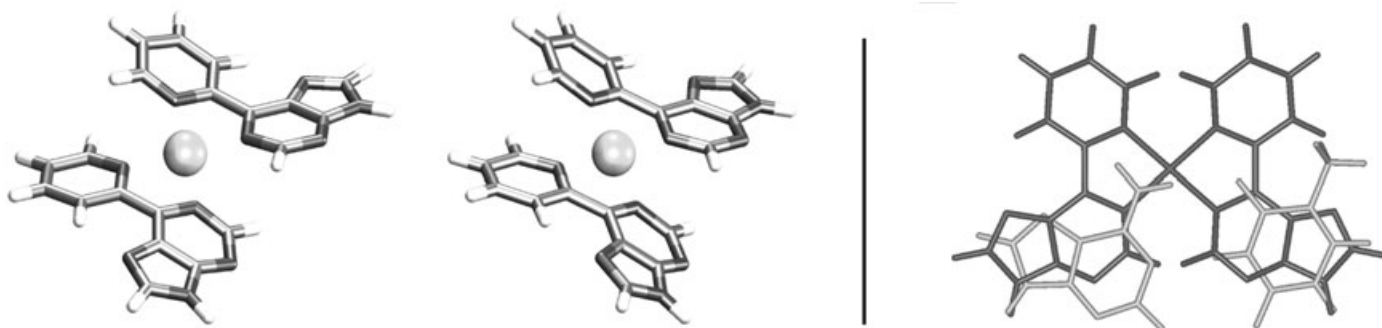


Figure 3. Left: Stereoview of the structure of $\text{Pur}^{\text{P}}\cdot\text{Ni}^{2+}\cdot\text{Pur}^{\text{P}}$ with optimized geometry obtained with Gaussian98.^[8] Right: Superposition of optimized $\text{Pur}^{\text{P}}\cdot\text{Ni}^{2+}\cdot\text{Pur}^{\text{P}}$ and A-T structures. The superposition was guided by Pur^{P} N9/A N9, Pur^{P} N9/T N1, and the hydrogen atoms attached to these nitrogen atoms.

involved in DNA replication, might recognize the $\text{Pur}^{\text{P}}\cdot\text{Ni}^{2+}$. Pur^{P} base pair. We are actively pursuing this possibility.

Received: September 21, 2004

Published online: January 28, 2005

Keywords: DNA · metallo base pairs · molecular switches · nickel · nucleobases

-
- [1] a) C. Switzer, S. E. Moroney, S. A. Benner, *J. Am. Chem. Soc.* **1989**, *111*, 8322–8323; b) J. A. Piccirilli, T. Krauch, S. E. Moroney, S. A. Benner, *Nature* **1990**, *343*, 33–47.
- [2] a) B. A. Schweitzer, E. T. Kool, *J. Am. Chem. Soc.* **1995**, *117*, 1863–1872; b) D. L. McMinn, A. K. Ogawa, Y. Q. Wu, J. Q. Liu, P. G. Schultz, F. E. Romesberg, *J. Am. Chem. Soc.* **1999**, *121*, 11585–11586.
- [3] a) E. Meggers, P. L. Holland, W. B. Tolman, F. E. Romesberg, P. G. Schultz, *J. Am. Chem. Soc.* **2000**, *122*, 10714–10715; b) H. Weizman, Y. Tor, *J. Am. Chem. Soc.* **2001**, *123*, 3375–3376; c) K. Tanaka, Y. Yamada, M. Shionoya, *J. Am. Chem. Soc.* **2002**, *124*, 8802–8803; d) T. Tanaka, A. Tengeji, T. Kato, N. Toyama, M. Shiro, M. Shionoya, *J. Am. Chem. Soc.* **2002**, *124*, 12494–12498; e) N. Zimmerman, E. Meggers, P. G. Schultz, *J. Am. Chem. Soc.* **2002**, *124*, 13684–13685; f) K. Tanaka, A. Tengeji, T. Kato, N. Toyama, M. Shionoya, *Science* **2003**, *299*, 1212–1213; g) C. Brotschi, C. J. Leumann, *Nucleosides Nucleotides Nucleic Acids* **2003**, *22*, 1195–1197.
- [4] Z. Kazimierczuk, H. B. Cottam, G. R. Revankar, R. K. Robins, *J. Am. Chem. Soc.* **1984**, *106*, 6379–6382.
- [5] M. Hocek, A. Holy, I. Vortuba, H. Dvořáková, *Collect. Czech. Chem. Commun.* **2001**, *66*, 483–499.
- [6] A. Lützen, M. Hapke, *Eur. J. Org. Chem.* **2002**, 2292–2297.
- [7] H. Hashimoto, M. G. Nelson, C. Switzer, *J. Am. Chem. Soc.* **1993**, *115*, 7128–7134.
- [8] *Gaussian98* (Revision A.7), M. J. Frisch, G. W. Trucks, H. B. Schlegel, G. E. Scuseria, M. A. Robb, J. R. Cheeseman, V. G. Zakrzewski, J. A. Montgomery, R. E. Stratmann, J. C. Burant, S. Dapprich, J. M. Millam, A. D. Daniels, K. N. Kudin, M. C. Strain, O. Farkas, J. Tomasi, V. Barone, M. Cossi, R. Cammi, B. Mennucci, C. Pomelli, C. Adamo, S. Clifford, J. Ochterski, G. A. Petersson, P. Y. Ayala, Q. Cui, K. Morokuma, D. K. Malick, A. D. Rabuck, K. Raghavachari, J. B. Foresman, J. Cioslowski, J. V. Ortiz, B. B. Stefanov, G. Liu, A. Liashenko, P. Piskorz, I. Komaromi, R. Gomperts, R. L. Martin, D. J. Fox, T. Keith, M. A. Al-Laham, C. Y. Peng, A. Nanayakkara, C. Gonzalez, M. Challacombe, P. M. W. Gill, B. G. Johnson, W. Chen, M. W. Wong, J. L. Andres, M. Head-Gordon, E. S. Replogle, J. A. Pople, Gaussian, Inc., Pittsburgh, PA, **1998**.
-